Single Cell Raman-Deuterium Isotope Probing for Drug Resistance of *Elizabethkingia* spp.

Shuying Yuan[1]*, Yanwen Chen[1]*, Yizhi Song[2]*, Lin Zou[3], Kaicheng Lin[2], Xinrong Lu[3], Ruijie Liu[1], Shaoxing Zhang[1], Danfeng Shen[3], Zhenju Song[4], Chaoyang Tong[4], Li Chen[3#], Guiqin Sun[1#]

[1]School of Medical Technology and Information Engineering, Zhejiang Chinese Medical University, Hangzhou, Zhejiang 310053, China.

[2]CAS Key Laboratory of Bio-Medical Diagnostics, Suzhou Institute of Biomedical Engineering and Technology, Chinese Academy of Sciences, Suzhou, Jiangsu 215163, China.

[3]Department of Medical Microbiology and Parasitology, Key laboratory of Medical Molecular Virology of Ministries of Education and Health, School of Basic Medical Sciences, Fudan University, Shanghai 200032, China.

[4]Department of Emergency Medicine, Zhongshan Hospital, Fudan University, Shanghai 200032, China.

#Corresponding author

Guiqin Sun: Email, sunguiqin2001@163.com

Li Chen: Email, lichen_bk@fudan.edu.cn

Abstract

Nosocomial infection associated with *Elizabethkingia* spp. is an emerging clinical

concern characterized by multi-drug resistance and severe clinical consequences particularly in immunocompromised individuals and infants. Efficient control of this infection demands quick and reliable methods to determine the right drugs for the treatment. In this study, *E. meningoseptica* ATCC 13253 and four clinical isolates of *Elizabethkingia* spp. obtained from China, were subjected to single cell Raman spectroscopy analysis coupling with deuterium probing (single cell Raman-DIP). The results demonstrated that single cell Raman-DIP could generate an antimicrobial susceptibility testing result for *Elizabethkingia* spp. colonies within 4 hours based on their metabolisms variations at single cell level, and the drug resistant spectra of *Elizabethkingia* spp. determined by single cell Raman-DIP were consistent with the classical MIC method. Meanwhile single cell Raman spectroscopy (single cell RS) was applied to analyze Raman spectra of *Elizabethkingia* spp., which were revealed that their ratios of nucleic acid/protein were lower than other gram-negative pathogens and isolates from different origins could be distinguished by their Raman fingerprint. The *in vitro* results confirmed that minocycline and levofloxacin are first-line antimicrobials for *Elizabethkingia* spp. infection.

Keywords: *Elizabethkingia* spp., single cell Raman spectroscopy deuterium isotope probing (single cell Raman-DIP), carbon-deuterium ratio (C-D ratio), normalized metabolic ratio, antimicrobial susceptibility test, minimum inhibitory concentration (MIC)

Introduction

The emergence and widespread distribution of antimicrobial resistant bacteria has led to an increasing concern with respect to potential environmental and public health risks. The crisis of antimicrobial resistant bacteria has been attributed to the overuse and misuse for medication (1). Therefore, it is important for clinicians to know the drug resistance of pathogens and use the suitable antimicrobials. In clinical practice, the bacterial drug resistance has been relied on phenotypic AST approaches, such as "minimum inhibitory concentration" (MIC) detected by broth microdilution method (BMD) (2, 3). At least 16-18 hours were taken by this method to detect the antimicrobial effects on bacterial population growth for isolated colonies. Rapid detection of microbial antimicrobial susceptibility could ensure the selection of effective antimicrobials and provide a reduction in total antimicrobial consumption (4).

Raman spectroscopy is a label-free, fast and non-destructive biochemical phenotype technology that been supplied to detect the vibration modes of molecules (5). Single cell RS provides a biochemical "fingerprint" of individual cell, which were reflected cell physiological and metabolic states (6). It was applied to identify bacterial strains (7-10) and to detect physiological changes during the treatment of antimicrobials (11, 12). It has been reported that different Raman spectra were consisted in *Listeria monocytogenes* with different susceptibilities to sakacin P in 2006 (13). Single cell RS analysis on different pathogens, including methicillin-resistant *Staphylococcus aureus*

(MRSA), *Enterococcus faecium*, *Enterococcus faecalis*, *Escherichia coli*, *Klebsiella pneumoniae*, *Pseudomonas aeruginosa*, *Acinetobacter baumannii*, *Serratia marcescens* and *Lactococcus lactis*, have been carried out (14-20).

It has been discovered that the metabolically active microorganisms could incorporate the deuterium (D) into the cells via NADH/NADPH electron transport chain, producing a newly formed carbon-deuterium (C-D) band in single cell RS analysis coupling with deuterium probing (single cell Raman-DIP) (5, 6, 21, 22). The occurrence of C-D band around 2040-2300 cm^{-1} has been recognized as antimicrobial resistance biomarker when bacteria were exposed to antimicrobials and D_2O (11). Recently, single cell Raman-DIP was proposed to achieve fast AST for pathogens such as *Escherichia coli*, *Klebsiella pneumoniae*, *Streptococcus mutans*, *Lactobacillus fermentum*, *Enterococcus faecalis and Staphylococcus aureus* (5, 23-26). However, the potential of single cell Raman-DIP application for fast AST for *Elizabethkingia* spp. has been undemonstrated.

Hospital infection associated with *Elizabethkingia* spp. is an emerging clinical concern characterized by multi-drug resistance and severe clinical consequences. Many cases of *Elizabethkingia* spp. infections have been reported as part of outbreaks in the state of Wisconsin (USA), London (UK) and Mauritius (27-29). *Elizabethkingia* spp. is a group of Gram-negative, none-ferment pathogens, responsible for a panel of diseases, including meningitis, sepsis, bacteremia, pneumonia, and neutropenic fever

(30-33).

In this study, the optimized single cell Raman-DIP was applied to four hospital-isolated *Elizabethkingia* spp. strains and a standard strain *Elizabethkingia meningoseptica* (EM) ATCC 13253. Unique features of *Elizabethkingia* spp. were revealed by that single cell RS, which were improved the tested might be used to differentiate *Elizabethkingia* spp. from the other pathogens. The MIC readout of *Elizabethkingia* spp. were given by single cell Raman-DIP within 4 hours and high consistent results were shown with gold standard. The possibility of applying single cell Raman-DIP for clinical diagnosis of *Elizabethkingia* spp. was demonstrated.

Materials and Methods

Microorganisms and growth conditions

Five *Elizabethkingia* spp. strains were used in this study, including ATCC 13253 ordered from American Type Culture Collection and four clinical isolates (FMS-007, HS-2, NB-46 and TZ-3) collected in China (34, 35). All strains were grown aerobically in Trypticase Soy Broth (TSB) (Sigma-Aldrich, America) at 35°C overnight and then seeded on blood agar plate (BioMérieux, France) for single colonies. The tested strains were confirmed by automated VITEK 2 Compact system with the Gram-Negative identification card (GN) (BioMérieux, France). The AST results were determined by single cell Raman-DIP and MIC, respectively.

111 **Single cell RS analysis of *Elizabethkingia* spp.**

112 Single colonies on blood agar plate were inoculated into 1 ml TSB and incubated at
113 35°C with 180 rpm for 16 h. Cells were washed with sterile deionized water three
114 times and resuspended in 10 ml sterile deionized water. After washing and
115 resuspending, 2.5 μL of cell suspension were transferred onto an aluminum-coated
116 slide (Sonopore, China). Raman spectra were obtained using WITec Alpha300R
117 confocal Raman microscope (WITec, Germany) with 532 nm excitations laser, 100×
118 magnifying dry objective (NA =0.9) (Carl Zeiss, Germany), 600 gr/mm grating. The
119 integration time per spectrum was 20 s and the power on the sample was 7-9 mW.
120 Spectrometry was measured for single cells spanning the range of 300-1,900 cm^{-1} to
121 cover the most relevant Raman peaks of microbial cells. The spectra of 5 strains were
122 analyzed with Principal component analysis (PCA) and linear discriminant analysis
123 (LDA) method in R software using FactoMineR package as described previously (24).
124 PCA was used to compress the information held by the spectra and the first 20
125 principal components that described the greatest variance of the spectral data were
126 used for LDA.

127

128 **MIC of *Elizabethkingia* spp. determined by broth microdilution method**

129 A standard assay (CLSI, 2019) was conducted in a 96-well microplate (Bio-kont,
130 China). The tested bacterial colonies on each blood agar plate were aseptically
131 transferred into Mueller-Hinton (MH) broth (BD Biosciences, America), and a
132 homogenous suspension with a density equivalent to a 0.5 McFarland's standard was

prepared. Then the bacterial suspension was diluted with MH broth at a ratio of 1:200. One hundred microliters of prepared bacterial solution were inoculated into wells with sequentially diluted antimicrobials and incubated at 35°C with 180 rpm for 16 h. Aztreonam, cefepime, imipenem, ticarcillin/clavulanic acid, piperacillin/tazobactam, amikacin, tobramycin, minocycline, levofloxacin and trimethoprim/sulfamethoxazole were used in this study. The concentrations of the ten antimicrobials were based on the breakpoints of other Non-Enterobacteriaceae listed in guidelines M100 (CLSI, 2019). MIC value and the results of antimicrobial susceptibility were interpreted based on guidelines M100 (CLSI, 2019).

Antimicrobial susceptibility detected by single cell Raman-DIP

D_2O (99% D atom, Sigma-Aldrich, US) labelling was performed following previous reported studies (6, 21). 3~5 isolated colonies selected from each blood agar plate were subjected to single cell Raman-DIP. Bacterial suspension preparation was prepared as the MIC detection. One hundred microliters of inoculated bacterial solution were added to each 96-well plates with standard concentrations of antimicrobial suggested in CLSI and incubated at 35°C with 180 rpm for 1 h. Sixty-six microliters 66 μL of D_2O was added to each well, and then incubated for two more hours. Cells were washed with sterile deionized water three times and resuspended in 50 μL of sterile deionized water. Two point five microliters of cell suspension were transferred onto an aluminum-coated slide. At least 20 to 30 single cell Raman spectra were obtained with 4 s integration time for each treatment. The

Raman spectra for carbon-deuterium (C-D) peaks (2040–2300 cm^{-1}) and carbon-hydrogen (C-H) peaks (2800–3100 cm^{-1}) were obtained respectively. The C-D ratio was calculated (C-D/C-D+C-H) and normalized (C-D ratio of treated group minus C-D ratio of no deuterium and no antimicrobials controls). The impact of a treatment was decided by the relative metabolic rate (relative C-D rate of the treatment was calculated by the ratio of normalized C-D of the treatment and the no drug control) (24). The cutoff reads for relative metabolic rate is 0.6 to separate the metabolism active (>0.6) and inhibited conditions (<0.6) for bacteria cultured under antimicrobial treatment (26).

Results

Single cell Raman spectral of *Elizabethkingia* spp.

The *Elizabethkingia* spp. strains used in this study were confirmed by biochemical characterization via automatic VITEK 2 Compact bacterial identification and drug sensitivity analysis system (data not shown). Raman spectra of five *Elizabethkingia* spp. strains and four ATCC Gram-negative reference strains (*Acinetobacter baumannii* ATCC 19606, *Escherichia coli* ATCC 25922, *Pseudomonas aeruginosa* ATCC 27853 and *Klebsiella pneumoniae* ATCC 700603) were measured and plotted in Figure 1A. Comparing with the other gram-negative strains, lower peaks in Raman spectra at around 780, 1479 and 1578 cm^{-1} were shown in *Elizabethkingia* spp. strains significantly. Raman peak at around 1450 cm^{-1} (assigned to protein) was chosen as a reference(36). The ratio of the peak intensity at 780, 1479 and 1578 cm^{-1} to 1450 cm^{-1}

were calculated and plotted in Fig 1B, 1C and 1D, respectively. The position of a Raman peak is represented its molecular structure while the intensity of the peaks is associated with the content of the molecule. Raman peaks at 780 cm^{-1} was assigned to cytosine and uracil structure, 1479 cm^{-1} was to guanine and adenine structure, 1578 cm^{-1} was assigned to guanine and adenine structure (37-39). The results of single cell RS implied that the ratio of nucleic acid/protein in *Elizabethkingia* spp. were significantly lower than the other four Gram-negative reference strains (Fig. 1).

Discrimination of *Elizabethkingia* spp. by single cell RS

Single cell RS of five *Elizabethkingia* spp. strains were analyzed through machine learning model LDA. The score of each spectrum on two most prominent components were illustrated in Fig. 2. It is clearly shown that the RS of five *Elizabethkingia* spp. strains were divided into two groups along the LD1 axis. One group mainly contained spectra from ATCC 13253, and the other group contained spectra from clinical strains (Fig. 2). ATCC 13253 was firstly isolated at Massachusetts in 1949 (40, 41), and the other four strains were recently isolated from China. It was indicated that single cell RS might provide a novel method for typing of *Elizabethkingia* spp. strains.

Rapid AST of Imipenem for *Elizabethkingia* spp. by single-cell metabolic activity

Single cell Raman-DIP was applied to measure metabolic activity of bacteria at single cell level (21). *Elizabethkingia* spp. strains were incubated in MH medium containing

198 40% of heavy water for 2 hours, the deuterium in the medium was incorporated in the
199 cellular biomass and produced a new peak at 2040-2300 cm^{-1} (C-D band) on the basis
200 of 2800-3100 cm^{-1} (C-H band) (Fig. 3A and 3D). Taken imipenem as an example to
201 detect metabolism under antimicrobials treatment using single cell Raman-DIP. After
202 exposed in imipenem, the intensity of C-D band in Strain FMS-007 was remained at
203 the same level of the drug-free control in which no imipenem was added (Fig. 3A),
204 then C-D ratio (Fig. 3B) and normalized C-D ratio (Fig. 3C) were calculated. This
205 was indicated that bacteria were still metabolic active under imipenem up to 16 ug/ml
206 and resulted in an MIC of above 16 ug/ml. Since 16 ug/ml was the resistant
207 breakpoint of *Elizabethkingia* spp. for imipenem, strain FMS-007 was regarded
208 resistant to imipenem. The C-D band of strain TZ-3 was not detected when imipenem
209 was presented at a concentration of 16 μg/ml (Fig. 3D, 3E and 3F), which meant the
210 bacterial metabolic activity was inhibited and the MIC could be determined as 16
211 ug/ml. The results showed that single cell Raman-DIP could be used to detect
212 microbial metabiotic activity and antimicrobial susceptibility of *Elizabethkingia* spp.
213

214 **The AST of *Elizabethkingia* spp. by single cell Raman-DIP**

215 The antimicrobial susceptibility of five *Elizabethkingia* spp. strains to ten
216 antimicrobials were tested by single cell Raman-DIP and classical MIC method. The
217 results by single cell Raman-DIP and MIC were summarized in Figure 4 and Table 1,
218 respectively. The breakpoints of antimicrobial susceptibility on guidelines M100
219 (CLSI, 2019) were used in this study.

The corresponding concentration of relative metabolic rate <0.6 was used to interpreted the result of antimicrobial susceptibility. In the AST results tested by single cell Raman-DIP, all five strains were resistant to seven antimicrobials (total tested ten antimicrobials), including aztreonam, cefepime, ticarcillin/clavulanic acid, piperacillin/tazobactam, amikacin, tobramycin and sulfamethoxazole/trimethoprim (Fig. 4). Except strain HS-2 was intermediate, they were resistant to imipenem. ATCC13253. HS-2, NB-46 and TZ-3 were sensitive to minocycline, while FMS-007 was intermediate. FMS-007 and TZ-3 was sensitive to levofloxacin, but ATCC 13253, HS-2 and TZ-3 were resistant. It implied that minocycline and levofloxacin were selectable drugs for *Elizabethkingia* spp. infection.

The antimicrobial susceptibility of five *Elizabethkingia* spp. strains were also tested by MIC, and the AST results between MIC and single cell Raman-DIP were compared (Table 1). The results of eight antimicrobials were consistent detected by single cell Raman-DIP and classical MIC method, including aztreonam, imipenem, ticarcillin/clavulanic acid, piperacillin/tazobactam, amikacin, tobramycin, minocycline and levofloxacin. However, the AST results of two methods were different in cefepime and sulfamethoxazole/trimethoprim. Five strains were all resistant to cefepime and sulfamethoxazole/trimethoprim tested by single cell Raman-DIP, but the results tested by MIC were sensitive or intermediate.

In this study, the results of antimicrobial susceptibility were similar between single cell Raman-DIP and MIC method. It took 4 hours to gain the AST results by single cell Raman-DIP, which was 4-5 times faster than MIC method. The results demonstrated that AST determined by single cell Raman-DIP was comparable to MIC, and single cell Raman-DIP was a practical complementation for MIC.

Discussion

Building a quick and reliable drug-resistance assay is an urgent clinical need for medical practice and public health. In this study, single cell Raman-DIP analysis was applied to measure the fingerprint and metabolic profile of *Elizabethkingia* spp. to a panel of antimicrobials. The isolates of *Elizabethkingia* spp. were responded high sensitivity to minocycline and levofloxacin confirmed by 4-hour single cell Raman-DIP procedure. It was consistent with previous reports (30, 35, 42-44). Our study on *Elizabethkingia* spp. was an addition to the previous single cell Raman-DIP application.

In few cases, the inconsistent susceptibility results were presented between single cell Raman-DIP and MIC method. Apart from cefepime and sulfamethoxazole/ trimethoprim, the other eight antimicrobials were showed the overall consistency rate of single cell Raman-DIP to 95%. Notably, in all inconsistent cases, the results given by single cell Raman-DIP were resistant while were sensitive or intermediate judged by MIC method which means they were no major errors. These results met the FDA

requirements (category agreement ≥90%, minor error ⩽10.0%, major error ≤3.0%, very major error ≤1.5%) (26). Inconsistent results were shown in cefepime and sulfamethoxazole/trimethoprim between single cell Raman-DIP and MIC. Cefepime works by inhibiting penicillin binding proteins essential to cell wall formation (45). A possible explanation for cefepime was that the replication of bacteria under the treatment of cefepime with concentration higher than MIC was inhibited, the cells were still metabolic active. Recently, the growth-arrested bacteria may still exhibit metabolic activity has been revealed on metabolism of *Mycobacterium tuberculosis* (46) and persister bacteria treated with antimicrobials (47). Sulfamethoxazole/trimethoprim is a competitive inhibitor of dihydropteroate synthase that was involved in DNA synthesis (48). However, the reason caused by sulfamethoxazole/trimethoprim was unclear. Single cell metabolic activity assessment via single cell Raman-DIP could provide new insights on antimicrobial administration to patients.

Single cell RS has already been used to identify *Mycobacterium tuberculosis* and yeast species (11, 12). In this study, the characteristic peaks of *Elizabethkingia* spp. on single cell RS were identified (Fig. 1). Comparing to the controls, the ratio of nucleic acid/protein (the ratio of the peak intensity at 780, 1479 and 1578 cm^{-1} to 1450 cm^{-1}) were significantly lower than the other gram-negative strains. The reason behind observation was required further multi-omics studies. In addition, clinical isolates of *Elizabethkingia* spp. from Chinese hospitals and reference strain ATCC 13253

286 isolated from Massachusetts were classified to two groups according to machine
287 learning model on single cell RS (Fig. 2). These results were indicated that single cell
288 RS could be used as a new and fast way for strain characterization.
289
290 The infection caused by *Elizabethkingia* spp. is a rare but life-threatening medical
291 condition (3). A critical challenger for clinician is to prescribe a useful antimicrobial
292 although strains are multidrug resistant. In this study, we demonstrated that single cell
293 Raman-DIP could achieve a rapid and reliable AST of *Elizabethkingia* spp. in 4 hours.
294 Single-cell RS combined with machine learning could distinguish *Elizabethkingia* spp.
295 from other gram-negative pathogens. Thus, great potential in *Elizabethkingia* spp.
296 related clinical studies and diagnosis were showed by single cell RS and single cell
297 Raman-DIP technique.
298
299 **Acknowledgments**
300 The authors would like to thank the funding support from the Natural Science
301 Foundation of Zhejiang Province (Y20C050003), National Natural Science
302 Foundation of China (31600644) and Department of Education of Zhejiang Province
303 (FX2020021).
304
305 **References**
306 1. Ventola CL. 2015. The antibiotic resistance crisis: part 1: causes and threats. P
307 T 40:277-83.

2. Brauner A, Fridman O, Gefen O, Balaban NQ. 2016. Distinguishing between resistance, tolerance and persistence to antibiotic treatment. Nat Rev Microbiol 14:320-30.

3. Balouiri M, Sadiki M, Ibnsouda SK. 2016. Methods for in vitro evaluating antimicrobial activity: A review. J Pharm Anal 6:71-79.

4. Kerremans JJ, Verboom P, Stijnen T, Hakkaart-van Roijen L, Goessens W, Verbrugh HA, Vos MC. 2008. Rapid identification and antimicrobial susceptibility testing reduce antibiotic use and accelerate pathogen-directed antibiotic use. J Antimicrob Chemother 61:428-35.

5. Tao Y, Wang Y, Huang S, Zhu P, Huang WE, Ling J, Xu J. 2017. Metabolic-Activity-Based Assessment of Antimicrobial Effects by D2O-Labeled Single-Cell Raman Microspectroscopy. Anal Chem 89:4108-4115.

6. Song Y, Cui L, Lopez JAS, Xu J, Zhu YG, Thompson IP, Huang WE. 2017. Raman-Deuterium Isotope Probing for in-situ identification of antimicrobial resistant bacteria in Thames River. Sci Rep 7:16648.

7. Colnita A, Dina NE, Leopold N, Vodnar DC, Bogdan D, Porav SA, David L. 2017. Characterization and Discrimination of Gram-Positive Bacteria Using Raman Spectroscopy with the Aid of Principal Component Analysis. Nanomaterials (Basel) 7.

8. Tang M, McEwen GD, Wu Y, Miller CD, Zhou A. 2013. Characterization and analysis of mycobacteria and Gram-negative bacteria and co-culture mixtures

by Raman microspectroscopy, FTIR, and atomic force microscopy. Anal Bioanal Chem 405:1577-91.

9. Schroder UC, Ramoji A, Glaser U, Sachse S, Leiterer C, Csaki A, Hubner U, Fritzsche W, Pfister W, Bauer M, Popp J, Neugebauer U. 2013. Combined dielectrophoresis-Raman setup for the classification of pathogens recovered from the urinary tract. Anal Chem 85:10717-24.

10. Kloss S, Kampe B, Sachse S, Rosch P, Straube E, Pfister W, Kiehntopf M, Popp J. 2013. Culture independent Raman spectroscopic identification of urinary tract infection pathogens: a proof of principle study. Anal Chem 85:9610-6.

11. Hilton SH, Hall C, Nguyen HT, Everitt ML, DeShong P, White IM. 2020. Phenotypically distinguishing ESBL-producing pathogens using paper-based surface enhanced Raman sensors. Anal Chim Acta 1127:207-216.

12. Wichmann C, Chhallani M, Bocklitz T, Rosch P, Popp J. 2019. Simulation of Transportation and Storage and Their Influence on Raman Spectra of Bacteria. Anal Chem 91:13688-13694.

13. Oust A, Moretro T, Naterstad K, Sockalingum GD, Adt I, Manfait M, Kohler A. 2006. Fourier transform infrared and raman spectroscopy for characterization of Listeria monocytogenes strains. Appl Environ Microbiol 72:228-32.

14. Assmann C, Kirchhoff J, Beleites C, Hey J, Kostudis S, Pfister W, Schlattmann P, Popp J, Neugebauer U. 2015. Identification of vancomycin

interaction with Enterococcus faecalis within 30 min of interaction time using Raman spectroscopy. Anal Bioanal Chem 407:8343-52.

15. Wang P, Pang S, Zhang H, Fan M, He L. 2016. Characterization of Lactococcus lactis response to ampicillin and ciprofloxacin using surface-enhanced Raman spectroscopy. Anal Bioanal Chem 408:933-41.

16. Dekter HE, Orelio CC, Morsink MC, Tektas S, Vis B, Te Witt R, van Leeuwen WB. 2017. Antimicrobial susceptibility testing of Gram-positive and -negative bacterial isolates directly from spiked blood culture media with Raman spectroscopy. Eur J Clin Microbiol Infect Dis 36:81-89.

17. Kwiatkowski P, Pruss A, Wojciuk B, Dolegowska B, Wajs-Bonikowska A, Sienkiewicz M, Mezynska M, Lopusiewicz L. 2019. The Influence of Essential Oil Compounds on Antibacterial Activity of Mupirocin-Susceptible and Induced Low-Level Mupirocin-Resistant MRSA Strains. Molecules 24.

18. Li J, Wang C, Shi L, Shao L, Fu P, Wang K, Xiao R, Wang S, Gu B. 2019. Rapid identification and antibiotic susceptibility test of pathogens in blood based on magnetic separation and surface-enhanced Raman scattering. Mikrochim Acta 186:475.

19. Fu S, Wang X, Wang T, Li Z, Han D, Yu C, Yang C, Qu H, Chi H, Wang Y, Li S, Tian B, Li W, Xia Z. 2020. A sensitive and rapid bacterial antibiotic susceptibility test method by surface enhanced Raman spectroscopy. Braz J Microbiol 51:875-881.

20. Liu TT, Lin YH, Hung CS, Liu TJ, Chen Y, Huang YC, Tsai TH, Wang HH,

374 Wang DW, Wang JK, Wang YL, Lin CH. 2009. A high speed detection
375 platform based on surface-enhanced Raman scattering for monitoring
376 antibiotic-induced chemical changes in bacteria cell wall. PLoS One 4:e5470.
377 21. Berry D, Mader E, Lee TK, Woebken D, Wang Y, Zhu D, Palatinszky M,
378 Schintlmeister A, Schmid MC, Hanson BT, Shterzer N, Mizrahi I, Rauch I,
379 Decker T, Bocklitz T, Popp J, Gibson CM, Fowler PW, Huang WE, Wagner M.
380 2015. Tracking heavy water (D2O) incorporation for identifying and sorting
381 active microbial cells. Proc Natl Acad Sci U S A 112:E194-203.
382 22. Wang Y, Song Y, Tao Y, Muhamadali H, Goodacre R, Zhou NY, Preston GM,
383 Xu J, Huang WE. 2016. Reverse and Multiple Stable Isotope Probing to Study
384 Bacterial Metabolism and Interactions at the Single Cell Level. Anal Chem
385 88:9443-9450.
386 23. Yang K, Li HZ, Zhu X, Su JQ, Ren B, Zhu YG, Cui L. 2019. Rapid Antibiotic
387 Susceptibility Testing of Pathogenic Bacteria Using Heavy-Water-Labeled
388 Single-Cell Raman Spectroscopy in Clinical Samples. Anal Chem
389 91:6296-6303.
390 24. Yi X, Song Y, Xu X, Peng D, Wang J, Qie X, Lin K, Yu M, Ge M, Wang Y,
391 Zhang D, Yang Q, Wang M, Huang WE. 2021. Development of a Fast
392 Raman-Assisted Antibiotic Susceptibility Test (FRAST) for the Antibiotic
393 Resistance Analysis of Clinical Urine and Blood Samples. Anal Chem
394 93:5098-5106.
395 25. Hong W, Karanja CW, Abutaleb NS, Younis W, Zhang X, Seleem MN, Cheng

JX. 2018. Antibiotic Susceptibility Determination within One Cell Cycle at Single-Bacterium Level by Stimulated Raman Metabolic Imaging. Anal Chem 90:3737-3743.

26. Zhang M, Hong W, Abutaleb NS, Li J, Dong PT, Zong C, Wang P, Seleem MN, Cheng JX. 2020. Rapid Determination of Antimicrobial Susceptibility by Stimulated Raman Scattering Imaging of D2O Metabolic Incorporation in a Single Bacterium. Adv Sci (Weinh) 7:2001452.

27. Perrin A, Larsonneur E, Nicholson AC, Edwards DJ, Gundlach KM, Whitney AM, Gulvik CA, Bell ME, Rendueles O, Cury J, Hugon P, Clermont D, Enouf V, Loparev V, Juieng P, Monson T, Warshauer D, Elbadawi LI, Walters MS, Crist MB, Noble-Wang J, Borlaug G, Rocha EPC, Criscuolo A, Touchon M, Davis JP, Holt KE, McQuiston JR, Brisse S. 2017. Evolutionary dynamics and genomic features of the Elizabethkingia anophelis 2015 to 2016 Wisconsin outbreak strain. Nat Commun 8:15483.

28. Moore LS, Owens DS, Jepson A, Turton JF, Ashworth S, Donaldson H, Holmes AH. 2016. Waterborne Elizabethkingia meningoseptica in Adult Critical Care. Emerg Infect Dis 22:9-17.

29. Issack MI, Neetoo Y. 2011. An outbreak of Elizabethkingia meningoseptica neonatal meningitis in Mauritius. J Infect Dev Ctries 5:834-9.

30. Burnard D, Gore L, Henderson A, Ranasinghe A, Bergh H, Cottrell K, Sarovich DS, Price EP, Paterson DL, Harris PNA. 2020. Comparative Genomics and Antimicrobial Resistance Profiling of Elizabethkingia Isolates

Reveal Nosocomial Transmission and In Vitro Susceptibility to Fluoroquinolones, Tetracyclines, and Trimethoprim-Sulfamethoxazole. J Clin Microbiol 58.

31. Lau SK, Chow WN, Foo CH, Curreem SO, Lo GC, Teng JL, Chen JH, Ng RH, Wu AK, Cheung IY, Chau SK, Lung DC, Lee RA, Tse CW, Fung KS, Que TL, Woo PC. 2016. Elizabethkingia anophelis bacteremia is associated with clinically significant infections and high mortality. Sci Rep 6:26045.

32. Lin JN, Yang CH, Lai CH, Huang YH, Lin HH. 2016. Draft Genome Sequence of Elizabethkingia anophelis Strain EM361-97 Isolated from the Blood of a Cancer Patient. Genome Announc 4.

33. da Silva PS, Pereira GH. 2013. Elizabethkingia meningoseptica: Emergent bacteria causing pneumonia in a critically ill child. Pediatr Int 55:231-4.

34. Sun G, Wang L, Bao C, Li T, Ma L, Chen L. 2015. Complete Genome Sequence of Elizabethkingia meningoseptica, Isolated from a T-Cell Non-Hodgkin's Lymphoma Patient. Genome Announc 3.

35. Sun G, Li M, Wang L, Guo H, Yu H, Chen J, Chen L. 2014. Clinical distribution and drug resistance of Elizabethkingia meningoseptica infection. Chinese Journal of Microecology 26:540-543.

36. Lau DP, Huang Z, Lui H, Man CS, Berean K, Morrison MD, Zeng H. 2003. Raman spectroscopy for optical diagnosis in normal and cancerous tissue of the nasopharynx-preliminary findings. Lasers Surg Med 32:210-4.

37. Stone N, Kendall C, Shepherd N, Crow P, Barr H. 2002. Near-infrared Raman

spectroscopy for the classification of epithelial pre-cancers and cancers. Journal of Raman Spectroscopy 33:564-573.

38. Stone N, Kendall C, Smith J, Crow P, Barr H. 2004. Raman spectroscopy for identification of epithelial cancers. Faraday Discuss 126:141-57; discussion 169-83.

39. Maquelin K, Kirschner C, Choo-Smith LP, van den Braak N, Endtz HP, Naumann D, Puppels GJ. 2002. Identification of medically relevant microorganisms by vibrational spectroscopy. J Microbiol Methods 51:255-71.

40. Brody JA, Moore H, King EO. 1958. Meningitis caused by an unclassified gram-negative bacterium in newborn infants. AMA J Dis Child 96:1-5.

41. King EO. 1959. Studies on a group of previously unclassified bacteria associated with meningitis in infants. Am J Clin Pathol 31:241-7.

42. Wang L, Zhang X, Li D, Hu F, Wang M, Guo Q, Yang F. 2020. Molecular Characteristics and Antimicrobial Susceptibility Profiles of Elizabethkingia Clinical Isolates in Shanghai, China. Infect Drug Resist 13:247-256.

43. Lin JN, Lai CH, Huang YH, Yang CH. 2021. Antimicrobial Effects of Minocycline, Tigecycline, Ciprofloxacin, and Levofloxacin against Elizabethkingia anophelis Using In Vitro Time-Kill Assays and In Vivo Zebrafish Animal Models. Antibiotics (Basel) 10.

44. Li W, Lin S, Luo F, Yu H, Sun G. 2020. Analysis of infection characteristics and drug susceptibility of Elizabethkingia meningoseptica nosocomial infection. Chinese Journal of Nosocomiology 30:327-330.

462 45. Yahav D, Giske CG, Gramatniece A, Abodakpi H, Tam VH, Leibovici L. 2020.
463 New beta-Lactam-beta-Lactamase Inhibitor Combinations. Clin Microbiol
464 Rev 34.
465 46. Ehrt S, Schnappinger D, Rhee KY. 2018. Metabolic principles of persistence
466 and pathogenicity in Mycobacterium tuberculosis. Nat Rev Microbiol
467 16:496-507.
468 47. Orman MA, Brynildsen MP. 2013. Dormancy is not necessary or sufficient for
469 bacterial persistence. Antimicrob Agents Chemother 57:3230-9.
470 48. Eyler RF, Shvets K. 2019. Clinical Pharmacology of Antibiotics. Clin J Am
471 Soc Nephrol 14:1080-1090.

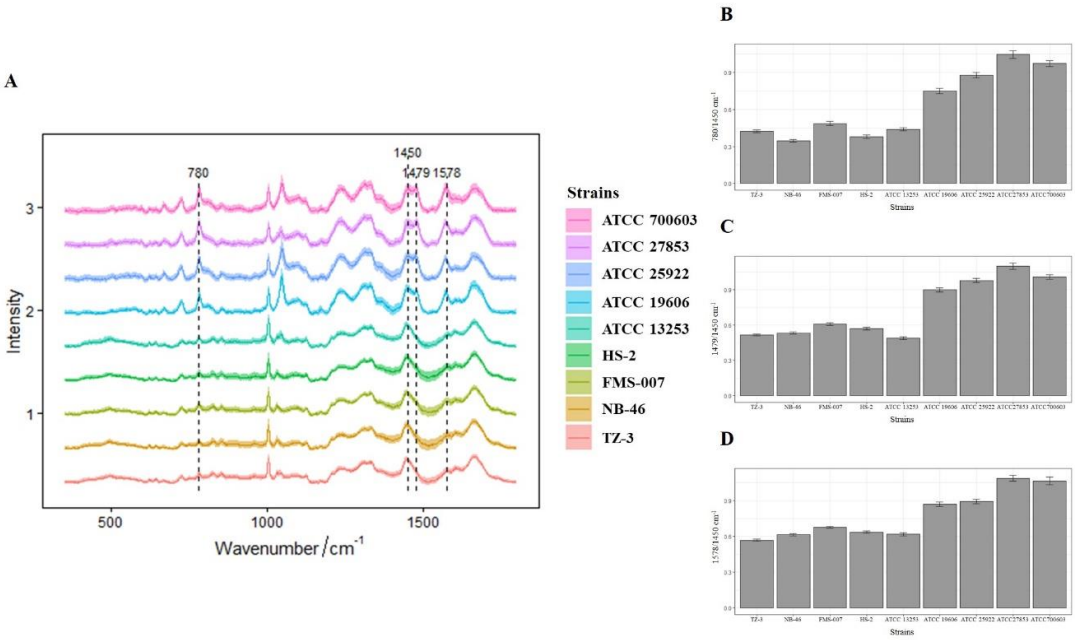

Figure 1 (A) Representative Raman spectra of five *Elizabethkingia* spp. strains and other four Gram-negative bacteria. (B) The ratio of nucleic acid peak at 780 cm^{-1} and protein peak at 1450 cm^{-1}. (C) The ratio of nucleic acid peak at 1479 cm^{-1} and protein peak at 1450 cm^{-1}. (D) The ratio of nucleic acid peak at 1578 cm^{-1} and protein peak at 1450 cm^{-1}.

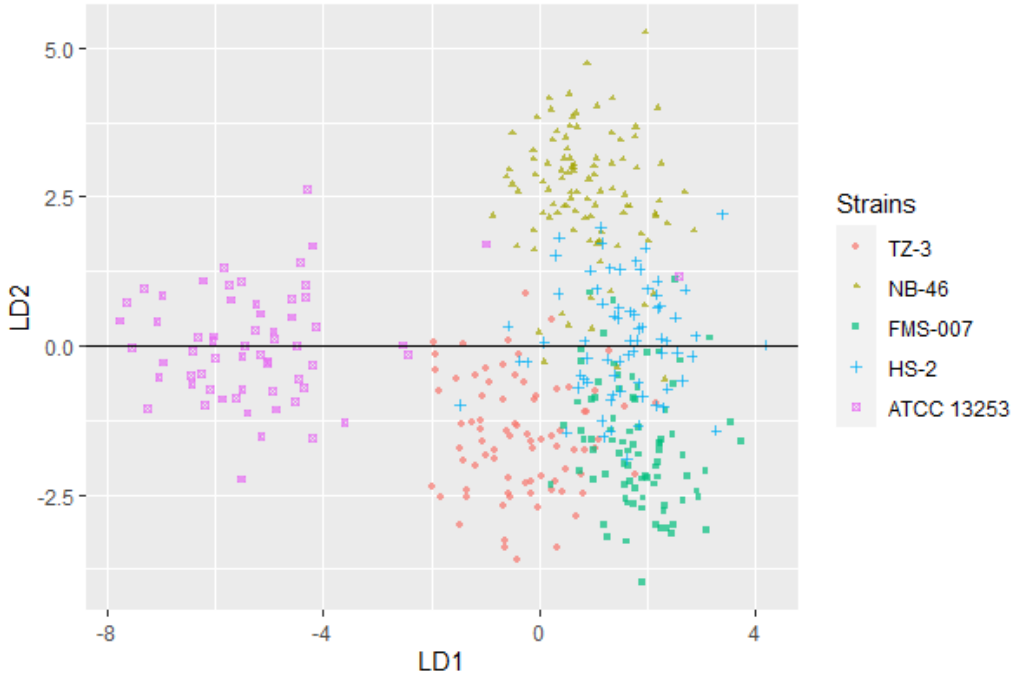

Figure 2 Two types of the five *Elizabethkingia* spp. strains. Each dot represented the combinative data of a single cell collected by single cell RS.

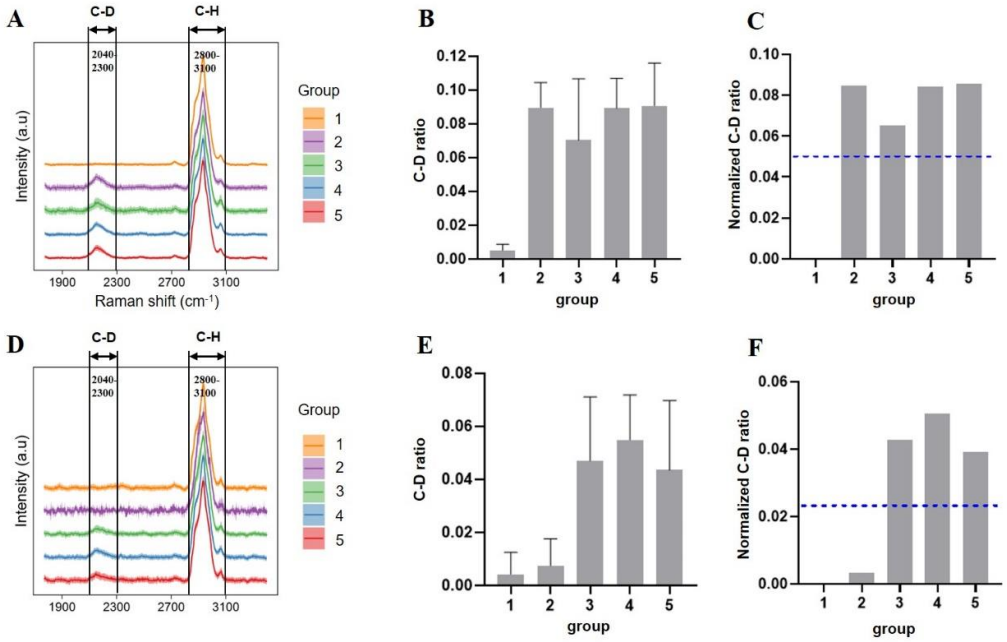

Figure 3 Raman spectra of cells treated with imipenem. (A) C-D and C-H band in FMS-007. (B) C-D ratio of FMS-007. (C) Normalized C-D ratio of FMS-007. (D) C-D and C-H band in TZ-3. (E) C-D ratio of TZ-3. (F) Normalized C-D ratio of TZ-3. The dotted lines in (B), (C), (E) and (F) indicate the cutoff value at 0.6 of the normalized C-D ratios. Group 1: without D_2O and imipenem; Group 2: D_2O with 16 ug/ml imipenem; Group 3: D_2O with 8 ug/ml imipenem; Group 4: D_2O with 4 ug/ml imipenem; Group 5: D_2O without imipenem.

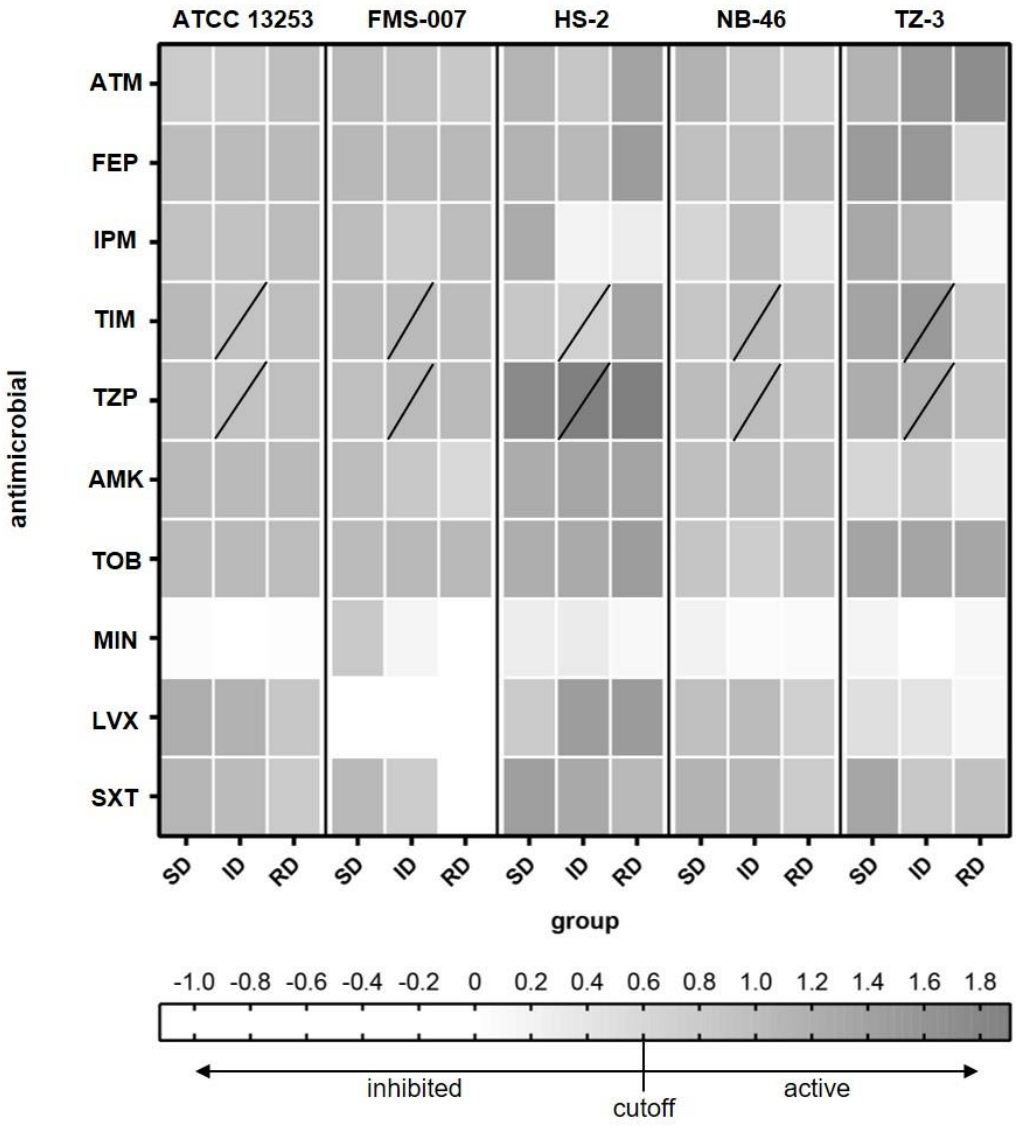

Figure 4 The relative metabolic rate of the five *Elizabethkingia* spp. strains determined by Raman-DIP. The antimicrobial concentrations of group SD, ID and RD were referenced by guidelines M100 (CLSI, 2019). SD: susceptible breakpoint corresponds antimicrobial concentration; ID: intermediate breakpoint corresponds antimicrobial concentration; RD: resistant breakpoint corresponds antimicrobial concentration; ATM: aztreonam; FEP: cefepime; IPM: imipenem; TIM: ticarcillin/clavulanic acid; TZP: piperacillin/tazobactam; AMK: amikacin; TOB: tobramycin; MIN: minocycline; LVX:

levofloxacin; SXT: sulfamethoxazole/trimethoprim. TIM and TZP were composed of two intermediate breakpoints (the data of lower concentration of intermediate breakpoints was shown);

Table 1 The antimicrobial susceptibility of five *Elizabethkingia* spp. strains

	ATCC13253		FMS-007		HS-2		NB-46		TZ-3		
Antimicrobial	MIC	Ram	MIC	Ram	MIC	Ram	MIC	Ram	MIC	Ram	MIC/Ram
ATM	R	R	R	R	R	R	R	R	R	R	R/R
FEP	I	R	S	R	I	R	I	R	S	R	S/R, I/R
IPM	R	R	R	R	I	I	R	R	R	R	R/R, I/I
TIM	R	R	R	R	R	R	R	R	R	R	R/R
TZP	R	R	R	R	R	R	R	R	R	R	R/R
AMK	R	R	R	R	R	R	I	R	R	R	R/R
TOB	R	R	R	R	R	R	R	R	R	R	R/R
MIN	S	S	I	I	S	S	S	S	S	S	S/S, I/I
LVX	R	R	S	S	R	R	I	R	S	S	S/S, R/R
SXT	S	R	S	R	R	R	S	R	I	R	S/R, I/R

MIC, minimum inhibitory concentration; Ram, single cell Raman-DIP; S, susceptible; I, intermediate; R, resistant; ATM: aztreonam; FEP: cefepime; IPM: imipenem; TIM: ticarcillin/clavulanic acid; TZP: piperacillin/tazobactam; AMK: amikacin; TOB: tobramycin; MIN: minocycline; LVX: levofloxacin; SXT: sulfamethoxazole/ trimethoprim.